

Structure Factor Scaling during Irreversible Cluster-Cluster Aggregation

F. Sciortino and P. Tartaglia

Dipartimento di Fisica, Università di Roma La Sapienza, Piazzale Aldo Moro 2, I-00185 Roma, Italy
(Received 29 April 1994)

We present a simple model to describe the evolution of the structure factor during irreversible diffusion limited cluster-cluster aggregation. For growing compact clusters, the scattered intensity is predicted to scale as in spinodal decomposition, i.e., as $q_m^d I(q/q_m)$. For fractal clusters, the scattered intensity is predicted to apparently scale in $q_m^{d_f} I(q/q_m)$ only in late stages. We find an excellent agreement with the experimental results of Carpineti and Giglio [Phys. Rev. Lett. **68**, 3327 (1992)] and with novel data from a dynamic simulation.

PACS numbers: 64.60.Cn, 05.40.+j, 82.70.Dd

Recently, very low angle static light scattering [1] and direct imaging [2] experiments on solutions of polystyrene spheres have addressed the issue of the spatial distribution of clusters during diffusion limited cluster-cluster aggregation (DLCA) [3]. Two unpredicted and puzzling results of these experimental works have stimulated a resurgence of interest in the cluster aggregation field and new connections with the dynamics of phase separation. Indeed, the results of [1] and [2] show that an (unexpected) spatial correlation among clusters arises as a result of an irreversible DLCA process, as revealed by the presence of a peak at a finite wave vector q_m in the scattered intensity $I(q, t)$. Even more interestingly, they also show that $I(q, t)$ at different late times can be superimposed if plotted as $q_m(t)^{d_f} I(q/q_m(t))$ vs q/q_m , i.e., in a form similar to the one observed in late stage spinodal decomposition once the space dimensionality d is substituted by the fractal dimension d_f , suggesting the presence of common elements between DLCA and phase separation.

In this Letter, we present a simple theory to explain the origin and the evolution of the experimentally detected cluster-cluster correlation during DLCA and discuss the relation with the late stage of spinodal decomposition. The two quantities we focus on are (i) the average number of clusters per unit volume $n(r, t)$ at distance r from the origin, knowing that one cluster is at the origin, and (ii) the size of the average cluster of mass $M(t)$ and radius $R(t)$ [4]. The time dependence of these two quantities is given by the following two coupled differential equations

$$\frac{\partial n}{\partial t} = D \nabla^2 n - \frac{n}{M} \frac{dM}{dt}, \quad (1)$$

$$\frac{dM}{dt} = D M S_d \left. \frac{\partial n}{\partial r} \right|_{r=2R(t)}, \quad M(t) = M(0) [R(t)/R(0)]^{d_f}, \quad (2)$$

with boundary conditions $n(R, t) = 0$ and $n(\infty, t) = n_0 M(0)/M(t)$ and initial conditions $n(r, 0) = n_0$ for $r \geq 2R(0)$. D is the diffusion coefficient which we assume to be mass dependent ($D \sim M^{-\gamma}$) and S_d is 2, $2\pi R$, $4\pi R^2$ in $d = 1, 2, 3$, respectively. Equation (1) indicates that $n(r, t)$ may change due to (i) diffusion in the pres-

ence of a concentration gradient or (ii) increase of the average cluster size (i.e., aggregation of clusters) [5]. Equation (2) reveals that the cluster radius increase is controlled by the mass flux at the boundary [6]. The moving boundary position is at $r = 2R(t)$, i.e., at the sum of the radii of the two coalescing clusters. The boundary conditions indicate that the cluster boundary $R(t)$ is sticky, in agreement with the assumption of irreversible aggregation, and that very distant clusters are randomly distributed in space. The initial conditions indicate that the system is homogeneous in space.

In the case of compact cluster structure (i.e., $d_f = d$), $n(r, t)$ and $M(t)$ can be calculated exactly, by writing $ds = D(M)dt$ and noting the analogy with the so-called moving boundary Stefan problem [7]. The solution is a function of the scaled variable $r/2s^{1/2}$ [8],

$$n(r, s) = n_0 \frac{M(0)}{M(s)} \left[1 - \frac{F(r/2s^{1/2})}{F(\lambda)} \right] \quad (3)$$

for $r \geq 2R(s)$ and $n(r, s) = 0$ for $r \leq 2R(s)$, where λ is a constant to be determined [9]. For $d = 1, 2$, and 3 , respectively, $F(x)$ is given by

$$F(x) = \operatorname{erfc}(x), \quad \operatorname{Ei}(-x^2), \quad \frac{e^{-x^2}}{x} - \sqrt{\pi} \operatorname{erf}(x). \quad (4)$$

The associated solution for the boundary motion is

$$R(s) = \lambda s^{1/2}. \quad (5)$$

Two important considerations are in order: (i) In all dimensions, $n(r, s)$ monotonically increases from zero at the sticky boundary to $n(\infty, t)$. Thus, a depletion region exists around each cluster. Since the nucleus growth is controlled by the same exponent as the growth of the depletion region, scaling in time is expected. (ii) From the relation between s and t we find $M(t) \sim t^{d/(2+\gamma d)}$, the same exponent predicted by the Smoluchowski approach for compact clusters [3].

$n(r, t)$ is by definition the product of the average number density times the radial distribution function [10]. The associated cluster structure factor is [10]

$$S(q, s) = 1 + \int [n(r, s) - n(\infty, s)] e^{iq \cdot r} dr. \quad (6)$$

At small q , $S(q, s)$ goes as q^2 , as imposed by mass conservation. Moreover, being $n(r, s)$ a function of the scaled variable $r/2s^{1/2}$, also $S(q, s)$ scales in time in $qs^{1/2}$ or, by Eq. (5), in $qR(s)$. The experimentally measured total scattered intensity $I(q, t)$ can be approximated as the product of the cluster form factor $P(q, t)$, well known for any d , and of the previously calculated $S(q, t)$. $P(q, t)$ is also a function of qR , i.e., of the same scaled variable of $S(q, t)$. This implies that the total scattered intensity will also be a scaled function of qR . Moreover, since $P(q, t)$ is proportional to the mass of the scatterer, a plot of $I(qR(t))/M(t)$ vs $qR(t)$ will show a remarkable data collapse, of the same kind as the one observed in late stage spinodal decomposition [11].

To test the model in detail for compact clusters we performed a Brownian dynamics (BD) simulation of a one-dimensional coagulating system [12]. We calculate the structure factor $S_{BD}(q, t)$, the cluster form factor $P_{BD}(q, t)$, and the total scattered intensity $I_{BD}(q, t)$ from the simulation, according to the following equations [13]:

$$I_{BD}(q, t) = \frac{1}{N} \left\langle \left| \sum_{i=1}^N e^{iqr_i(t)} \right|^2 \right\rangle, \quad (7)$$

$$S_{BD}(q, t) = \frac{1}{n_c(t) \langle M^2 \rangle} \left\langle \left| \sum_{k=1}^{n_c(t)} m_k e^{iq[r_{cm_k}(t)]} \right|^2 \right\rangle, \quad (8)$$

$$P_{BD}(q, t) = \frac{1}{N} \left\langle \sum_{k=1}^{n_c(t)} \left| \sum_{i=1}^{m_k} e^{iqr_i(t)} \right|^2 \right\rangle, \quad (9)$$

where $r_i(t)$ is the position of the i th monomer, $r_{cm_k}(t)$ and m_k are, respectively, the center of mass and mass of cluster k , and $n_c(t)$ is the number of clusters at time t .

Figure 1 shows S_{BD} compared with the theoretical predictions, Eqs. (3)–(6). The inset shows the comparison in real space. As predicted by Eq. (3) the data from the simulation collapse on the same curve once plotted as

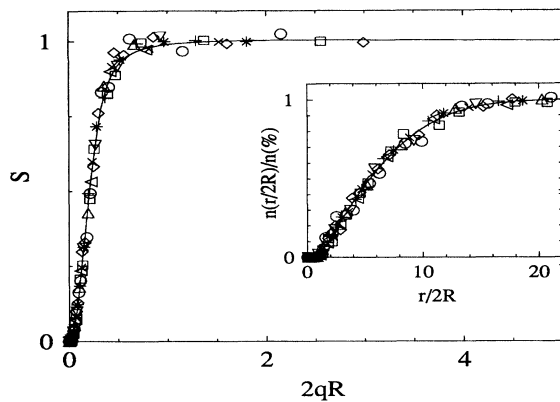


FIG. 1. $S(q, t)$ as a function of the scaling variable $2qR(t)$. The full line is the analytical prediction of Eq. (4), while the symbols are from the $d = 1$ BD simulation. The time interval spans 10^7 integration steps. Polydispersity has been taken into account increasing the cluster density in the analytical solution by $\langle M^2 \rangle / \langle M \rangle^2$. The inset shows the corresponding profile of $n(r, t)$ in the scaled variable $r/2R(t)$.

a function of the scaled variable $qR(t)$ or $r/R(t)$. The agreement is excellent, especially if one considers that there are no adjustable parameters. Symbols in Fig. 2 are $I_{BD}/M(t)$ as a function of the scaled variable $2qR(t)$, while the full line is the product of $S(q, t)$ shown in Fig. 1 times $P(q, t)$. $P(q, t)$ is calculated averaging the form factor of a $d = 1$ compact cluster over the polydispersity obtained from the BD simulation. The experimental data and the analytical solutions for $S(q, t)$ and $P(q, t)$ are shown in a log-log scale in the inset. It is worth noting that $P(q, t)$ controls the behavior of the scattered intensity to the right of the peak, while $S(q, t)$ is responsible for the low q limit. Another important consideration stems from the fact that the scaled $P(q, t)$ is independent from the initial number density n_0 . Instead, the ratio between the cluster density and n_0 does change the scaled $S(q, t)$. Thus the scaling function for $I(q, t)$ will depend on n_0 .

When the growing cluster is a fractal $dM/dt \sim R^{(d_f-1)}dR/dt$ and does not cancel any longer the surface term on the right-hand side of Eq. (2). The addition of the extra R^{d_f-d} term changes the time dependence of the cluster growth compared to the time dependence of the growth of the depletion region. As a consequence, the $n(r, t)$ profile does not scale anymore with $R(t)$ (see the inset of Fig. 3), and we are forced to analyze the model solving numerically Eqs. (1) and (2). Before doing so, we note that while in the nonfractal case the average density of the cluster does not change during the aggregation, in the case of fractal clusters the density decreases with R^{d_f-d} . Thus, there is a time t_f , and an associated radius R_f , at which the average density reaches the value of the initial density. When $R = R_f$ clusters fill the space completely, and the growth process stops. We also note that the structure of Eqs. (1) and (2) does not change when written in terms of the dimensionless variable r/R_f . Thus, the model predicts that at constant $R(t)/R_f$ one should observe the same scattering pattern, independently from n_0

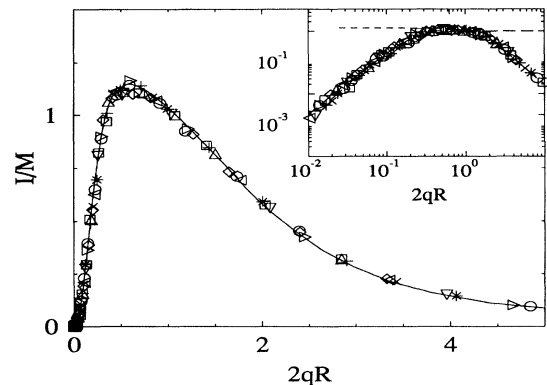


FIG. 2. Scaled intensity as a function of the scaling variable $2qR(t)$. Full line is the theoretical prediction while the symbols are from the BD simulation. The inset shows I_{BD} in log-log scale. The dotted line is $P(2qR(t), t)/M(t)$ while the long-dashed line is $S(2qR(t), t)$.

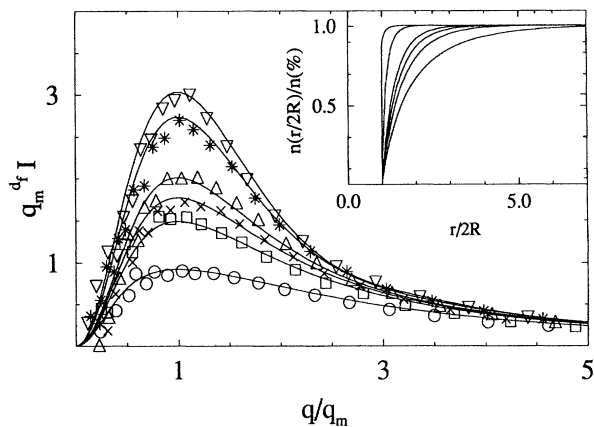


FIG. 3. Scaled $I(q, t)$ at different times during the aggregation process in the *non-scaling* regime. Symbols are redrawn from [1]. The full lines are the prediction of the model. The inset shows the corresponding $n(r, t)$ functions, to highlight the absence of scaling in $r/2R$. Note also that the last $n(r/2R(t))$ can be well approximated with a step function centered at $r = 2R$.

[14]. From the numerical solution we find the following: (i) During the initial stage of the growth process (when the inter cluster distance is much bigger than the cluster size), the flux of matter at R is proportional to R^{d-2} , as in the Euclidean case. Under such conditions, from Eq. (2) one has $R^{d_f-1}dR/ds \sim R^{d-2}$, or R going as $s^{1/(d_f-d+2)}$ and $M \sim t^{d_f/[d_f(1+\gamma)-(d-2)]}$, the same exponent predicted by the Smoluchowski approach for fractal clusters [3]. (ii) On increasing the time the inter cluster distance becomes comparable with the cluster size. In this late-stage regime, the profile of $n(r)$ becomes very similar to a step function centered at $r = 2R$, and the cluster radius appears as the relevant length. Thus, an apparent scaling in $qR(t)$ is again expected close to freezing.

We now compare the predictions of our model with the experimental results of Carpineti and Giglio [1] on aggregation of polystyrene spheres in water. They observe the formation of clusters with $d_f \approx 1.9$ for $d = 3$. The scattered intensity shows a well defined peak that moves in time. The kinetic process is separated in three regions: an initial region where no scaling in $q_m^{d_f} S(q/q_m)$ is observed (symbols in Fig. 3), an intermediate region where scaling is observed (symbols in Fig. 4), and a saturation region where no further change in the dynamical structure factor is observed. To calculate $S(q, t)$ we numerically solve Eqs. (1) and (2) for $d_f = 1.9$. For $P(q, t)$ we use a standard Fisher-Burford form [15]. The total scattered intensity, $I(q, t) = S(q, t)P(q, t)$, at selected times is shown in Fig. 3 and compared with the data from Ref. [1]. The corresponding $n(r/R(t), t)$ functions, to be compared with the inset of Fig. 1, are reported in the inset to show the progressive evolution toward a step function. Indeed, in these late stages

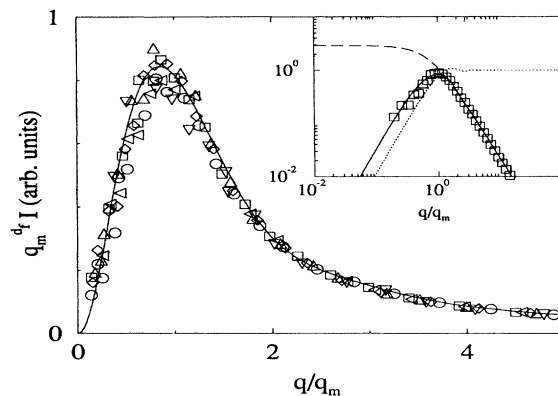


FIG. 4. Scaled $I(q, t)$ at different times during the aggregation process in the *scaling* regime. Symbols are redrawn from [1]. The full line is the prediction of the model when the $n(r)$ function can be approximated via a step function. The inset shows $I(q)$, $S(q)$, and $P(q)$ in log-log scale. Squares are experimental data in the scaling regime (courtesy of M. Carpineti and M. Giglio).

the final $q_m^{d_f} I(q/q_m)$ are coincident within a few percent with the $q_m^{d_f} I(q/q_m)$ obtained approximating $n(r, t)$ with a step function. The final $q_m^{d_f} I(q/q_m)$ is shown with the experimental data [1] for the late stage scaling region in Fig. 4 [16]. In the inset the decomposition of the $I(q, t)$ in its structure and form factor parts is presented.

In conclusion, we have proposed a simple model for the cluster spatial correlation during DLCA. A peak in $I(q, t)$ is shown to arise from the formation of a depletion zone around the growing clusters [17]. The exponents z controlling the time dependence of the mass are also obtained. Differently from the Smoluchowski equations [18], no *a priori* evaluation of the reaction rates kernels is required, but only information on d_f . The model shows that true scaling, during the whole aggregation process, is observed only for compact growing clusters where correlations have the same scaling behavior as the size of the growing cluster. In both quantities, distance scales with reduced time s as $s^{1/2}$. Under such conditions, the $I(q, t)$ can be scaled as $I(qR, t) \sim M(t)F(qR) \sim R(t)^d F(qR)$. The function $F(qR)$ is not universal, but depends on the difference in density of the cluster compared to the bulk density. For growing fractal clusters, no true scaling is predicted. The reason for such difference is shown to arise from the different time scale of $R(t)$ and $n(r, t)$. Only close to gelation, the growth of the cluster takes over the diffusional process, and an apparent scaling is observed. In this limit $I(qR, t) \sim R(t)^{d_f} F(qR)$.

The theory we propose here only allows us to study processes where a typical cluster size does exist, and it is not thus immediately extended to cluster aggregation in reaction limited regime (RLCA). This notwithstanding, we do expect that the presence of an activation energy for aggregation, which would reflect in our model in the

modification of the boundary conditions from sticky to partially reflecting, will cause the squeezing of $S(q, t)$ toward $q = 0$. On moving from DLCA toward RLCA the $I(q)$ peak position will thus shift toward smaller and smaller q values, eventually moving out from the available experimental window. Such behavior has been recently observed [2,19].

In the end, it is worth pointing out the relations between irreversible coagulation and phase separation. Irreversible aggregation can be seen as a phase separation process in deep quench limit (from infinite to zero temperature), when separation proceeds only along a path of decreasing total energy and cluster breaking is very rare. In such conditions, mechanisms like the evaporation-condensation are less effective than diffusion and coalescence of the entire clusters. Indeed, the $M(t)$ dependence we find is the same obtained from the Binder-Stauffer diffusion-reaction mechanism for droplet coarsening [20], without imposing any *ad hoc* requirement of self-similarity in the droplet configuration. The q^2 and q^{-4} limit in $I(q, t)$ in the late stage decomposition in deep quench also coincides with the $I(q, t)$ behavior during aggregation predicted by our model in three dimensions. Our exact results suggest that the scaling function depends strongly on the initial conditions and coarsening process.

We thank A. Belloni, M. Carpineti, and H. Larralde for helpful discussions. This work was supported in part by grants from the INFM-MURST and the GNSM-CNR.

-
- [1] M. Carpineti and M. Giglio, Phys. Rev. Lett. **68**, 3327 (1992).
- [2] D.J. Robinson and J.C. Earnshaw, Phys. Rev. Lett. **71**, 715 (1993).
- [3] For a general review see, e.g., T. Vicsek, *Fractal Growth Phenomena* (World Scientific, Singapore, 1989); P. Meakin, in *The Fractal Approach to Heterogeneous Chemistry*, edited by D. Avnir (Wiley, New York, 1989); several articles in *On Growth and Form*, edited by H.E. Stanley and N. Ostrowsky, (M. Nijhoff Publishers, Dordrecht, The Netherlands, 1986); D.A. Weitz and M. Oliveria, in *Kinetics of Aggregation and Gelation*, edited by F. Family and D.P. Landau (North-Holland, Amsterdam, 1984).
- [4] We neglect polydispersity, since in DLCA regime a characteristic average cluster mass exists.
- [5] Equation (1) is the standard diffusion equation $\partial c(r, t)/\partial t = D\nabla^2 c(r, t)$, where $c(r, t) = n(r, t)M(t)$ is the mass concentration, expressed in the $M(t)$ and $n(r, t)$ variables.
- [6] See, for example, W.B. Russel *et al.*, *Colloidal Dispersions* (Cambridge Univ. Press, Cambridge, 1989), p. 268.
- [7] J. Crank, *The Mathematics of Diffusion* (Oxford Univ. Press, Oxford, 1956); H.S. Carslaw and J.C. Jaeger, *Conduction of Heat in Solids* (Oxford Univ. Press, Oxford, 1959).
- [8] The solutions are valid when $R(t) \gg R(0)$.
- [9] The unknown λ in Eqs. (3)–(5) can be obtained by plugging the solution for $n(r, s)$ and $R(s)$ in Eq. (2) and solving the resulting equation. Thus λ depends only on the ratio between the cluster density and n_0 .
- [10] J.P. Hansen and I.R. McDonald, *Theory of Simple Liquids* (Academic Press, London, 1986).
- [11] For a general review on spinodal decomposition see, e.g., J.D. Gunton, M. San Miguel, and P.S. Sahni, in *Phase Transition and Critical Phenomena*, edited by C. Domb and J.L. Lebowitz (Academic Press, New York, 1983), Vol. 8, p. 267.
- [12] We simulate a coagulating system of $N = 10^5$ monomer of length one on a $d = 1$ lattice of length $L = 10^6$. Monomers are allowed to evolve in time performing BD, with time step 0.01. At each step, touching clusters are joined irreversibly to form a new cluster of mass equal to the sum of the old masses and length equal to the sum of the length of the previous clusters. D has been kept constant [$D(M) = 1$]. As expected, we find that the average mass increases with time as $M \sim t^{1/2}$ and the cluster size distribution evolves toward a scaled function of the average cluster size [J.A. Marqusee, Phys. Rev. A **35**, 1856 (1987)].
- [13] Quantities in Eqs. (8) and (9) are defined consistently with $S(q, t)$ of Eq. (6) to take into account the point nature of the scatterers and the presence of polydispersity.
- [14] This prediction has been recently confirmed: see M. Carpineti, M. Giglio, and V. Degiorgio, Phys. Rev. E **51**, 589 (1995).
- [15] The Fisher-Burford (FB) form gives a good representation of the experimental form factor. See D. Asnaghi *et al.*, Phys. Rev. A **45**, 1018 (1992). We relate the gyration radius R_g in the FB expression to $R(t)$ according to $R_g^2 = (3 - d_f + d)/(5 - d_f + d)R(t)^2$.
- [16] In the late stage regime [in which the z exponent can be extracted from the experimental data being $I(q, t) \sim M(t)$] $z = 1$, in agreement with our model when for γ the hydrodynamic regime value $1/d_f$ is chosen.
- [17] G.P. Banfi *et al.*, Phys. Rev. Lett. **69**, 3401 (1992).
- [18] M. von Smoluchowski, Phys. Z. Sowjetunion **17**, 557 (1916).
- [19] M. Carpineti and M. Giglio, Phys. Rev. Lett. **70**, 3828 (1993).
- [20] K. Binder and D. Stauffer, Phys. Rev. Lett. **33**, 1006 (1974).